DOI 10.2478/igbp-2013-0001 PAPERS on GLOBAL CHANGE, 20, 29–45, 2013

VARIABILITY TO SEDIMENTARY DYNAMICS AND CLIMATIC CONDITIONS DURING THE LAST TWO MILLENNIA AT SEBKHA SOUASSI IN EASTERN TUNISIA

ELHOUCINE ESSEFI[a,b], HAYET BEN JMAA[c,d], JAMEL TOUIR[e,f], MOHAMED ALI TAGORTI[g], CHOKRI YAICH[a,b]

[a] National Engineering School of Sfax, Road of Soukra, km 4 Zip code 3038, University of Sfax, Road of the Airport km 0.5, Zip code: 3029, Tunisia.

[b] RU: Sedimentary Dynamics and Environment (DSE) (Code 03/UR/10-03), National Engineering School of Sfax, University of Sfax, Tunisia.
e-mail: hocinsefi@yahoo.fr

[c] Faculty of Arts and Humanities of Sfax, Road of the Airport 5, Zip code 3023, University of Sfax, Tunisia.

[d] Laboratory of Geomorphologic Cartography of Fields, Environments, and Dynamics, Tunisia.

[e] Laboratory of Water Energy and Environment, National Engineering School of Sfax, University of Sfax, Tunisia.

[f] Faculty of Sciences of Sfax, Road of Soukra km 4, Zip code 3038 Sfax, University of Sfax, Tunisia.

[g] Higher Institute of Biotechnology of Monastir, Tahar Haded Avenue, Zip code 5000, Monastir; University of Monastir. Road Sallem Bechir – B.P. n° 56 – 5000 Monastir, Tunisia.

ABSTRACT: This paper covers work intended to study the interplay of sedimentary dynamics and climatic variability over the last two millennia within Tunisia's sebkha Souassi. Based on the Visual Core Description, and magnetic susceptibility, we date the core from sebkha Souassi to the last two millennia. Genetic grain-size distribution then provided a basis for the identification of six climatic stages, i.e. the Warming Present

(WP), the Late Little Ice Age (Late LIA), the Early Little Ice Age (ELIA), the Medieval Climatic Anomaly (MCA), the Dark Ages (DA), and the Roman Warm Period (RWP). The WP stretches across the uppermost 3 cm, with a high grey scale indicating a dry climate. The Late LIA is located between 3 and 7 cm, and the ELIA between 7 and 28 cm. Intermediate values for GS indicate that this stage may be classified as moderate. The MCA spanning from 28 to 40 cm is marked by a sharp decrease in GS indicative of a wet period. The DA appear along the part between 40 and 79 cm, a shift from light to dark sediments being recorded. The RWP in turn appears between 79 and 114 cm. Based on the grain-size distribution, two low-frequency cycles were identified, indicating radical global changes in climatic conditions, differential tectonics and groundwater fluctuations. High-frequency cycles in turn attest to local modifications of climatic conditions.

KEY WORDS: last two millennia, climatic stages, sedimentary dynamics, sebkha Souassi, Tunisia.

INTRODUCTION

As was anticipated by previous studies (Essefi 2009, Essefi *et al.* 2009, Essefi *et al.* 2012c, Tagorti *et al.* 2013), the record as regards climatic variability does not change the sedimentary and hydric filling of sebkha Souassi radically, the signal of climatic change being drowned in the homogeneity imposed by a stable hydrogeological context (Tagorti *et al.* 2013, Essefi 2013). In addition, the sedimentary dynamics along the watershed of the depression are also controlled by groundwater involvement (Essefi *et al.* 2013).

The work described in this paper has therefore sought to infer sedimentary dynamics and climatic variability over the last two millennia by reference to grain-size distribution. In addition, to set the core within a chronological framework, visual description was applied (in comparison with the sebkha Mhabeul core), and magnetic properties were also studied (by detection of tephra layers).

Prior to any destructive analysis being embarked upon, non-destructive analysis in the form of **V**isual **C**ore **D**escription (VCD) is able to supply a great deal of information about core content, texture, and the organization of sedimentary bands. Furthermore, it may be an efficient tool for correlating different cores from the same playa or different playas, with a view to these being compared and their stratigraphy established. In this study, VCD was carried out with a special focus on three reference sandy bands detected visually in the core collected from sebkha Souassi, as well as the so-called grey-scale variability (Rodbell *et al.* 1999). In order to infer climatic variability over the last two millennia, a correlation between a core from sebkha Souassi and a core from sebkha Mhabeul, southeastern Tunisia (Marquer *et al.* 2008) was worked on, with account being taken of grey-scale variability, as well as the three reference sandy bands also detected within a 65 cm core from sebkha Mhabeul (Marquer *et al.* 2008).

THE STUDY AREA

The sebkha of Souassi is part of the sebkha of Sidi El Hani, which is in turn part of the Mechertate-Chrita-Sidi El Hani system. The sebkha of Sidi El Hani is an elongate NW-SE depression in the Sahel area (eastern Tunisia), which has a relatively small drainage basin (Fig. 1). By no means does it connect with the sea, though it does contain huge quantities of salt across tens of kilometres. It is fed by temporary and permanent hydrological networks (Oued Maktaa and Oued Chrita respectively) − Figure 1, and represents the basal part of the endorheic Sidi El Hani-Chrita-Mechertat system (Fig. 1) (Ben Jmaa, 2008). The sebkha of Sidi El Hani consists of three communicated playas. From north to the south, we find the playas of Sidi El Hani (*sensu stricto*), the playa of Souassi and the playa of Dkhila. Topographically, the sebkha of Souassi is limited by various hills that barely exceed 100 m in altitude. This topographic contrast helps to create a developed hydrological network within the 3300 km^2 of its hydrological basin, on which many dams have been constructed (Fig.1). The three components of sebkha Sidi El Hani have different orientations. The Sidi El Hani (*sensu stricto*) and Dkhila playas have an N 170 orientation; that of Souassi N 90.

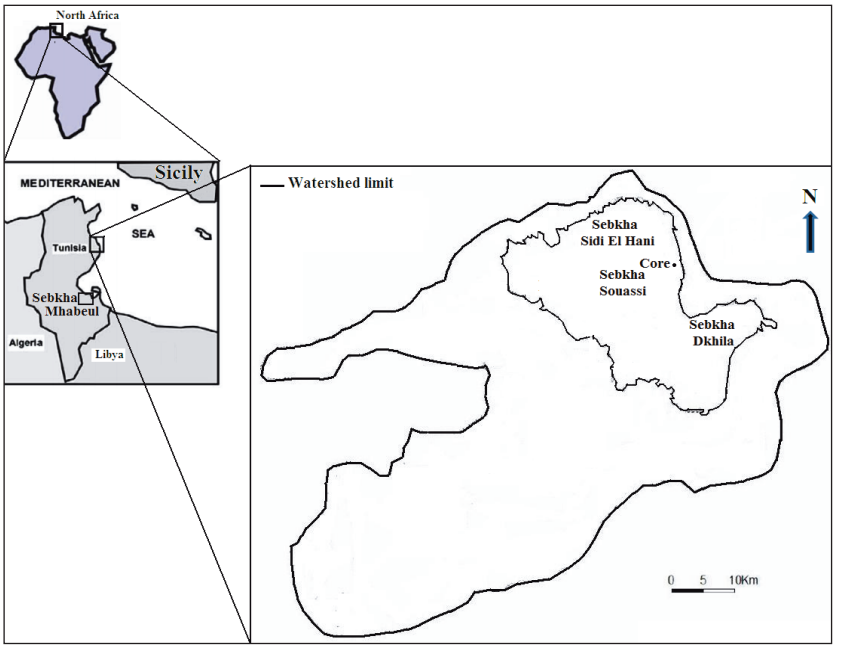

Figure 1. Geographical location of sebkha Souassi and sebkha Mhabeul

The sebkha of Mhabeul (southeast Tunisia) is an inland saline environment (Fig. 1). This depression records the climatic variability present over the last two millennia (Marquer *et al.* 2008). Since it is the only known site recording both climatic variability

and sedimentary dynamics over the most recent millennia, this sebkha serves as a reference example from which to infer the record of major climatic events within similar depressions (e.g., Essefi 2009). Like sebkha Souassi, this inland depression is also characterized by a groundwater involvement (the water table being less than 0.5 m below the surface).

METHODS AND MATERIALS

The coring technique is found to be one of the efficient ways in which to study both sedimentary dynamics and the record of climatic variability (Essefi 2009, Essefi *et al.* 2012a). This is done by means of the laboratory analyses to which collected cores were subjected, these being both destructive (VCD) and non-destructive (magnetic study and grain-size analysis).

After Marquer *et al.* (2008), an arbitrary method was used in this study to evaluate darkness on the basis of a grey scale (GS). It is worth noting that the concept of the grey scale is related to colour; but the grey scale is a relative concept within the same core. The same colour may have different grey-scale values depending on which of the studied cores it originates from. For instance, a grey band is attributed to a high grey-scale value if it is located within a core dominated by pale colours. This same grey band may be attributed a low grey-scale value if it is located within a core dominated by dark colours. Furthermore, the grey scale adopted in this study is the inverse of the scale used by Marquer *et al.* (2008). This reflects the fact that it is more logical to have a GS correlated, rather than anti-correlated, with darkness. The scale in question assumes values in the range 0-10, with pale sediment given a value of 0 and black sediment 10. The GS is in fact taken as a proxy for the nature and intensity of flooding events due to meteoric water (Rodbell *et al.* 1999). Minimum grey-scale values are associated with high-magnitude floods, hence characterizing periods during which high-intensity precipitation events occurred at high frequency, most probably during wet seasons. Maximum grey-scale values are associated with more stable climatic conditions, marked by flood events of lower magnitude and/or lower frequency.

Cores were also investigated in terms of genetic grain-size distributions. Wet process analyses were carried out using a FRITSCH laser grain-size analyzer. This investigation distinguished between the eolian, geochemical and hydraulic sedimentations on the basis of modal values for of grain-size distribution (Sun *et al.* 2002, Allen and Haslett 2006, Manté *et al.* 2007, Essefi 2009, Essefi *et al.* 2013). Sun *et al.* (2002) considered the fraction centered around 6 μm as the fine eolian component, and the fraction centered around 60 μm as the coarse eolian component. The coarse hydraulic component is in turn centered around 380 μm, and the fine hydraulic fraction around 1 μm. On the basis of the cumulative curves they developed, Tricart and Cailleux (1962) distinguished between 23 types of sedimentation: six estuary and deltaic, seven marine, two glacial,

three eolian and five fluvial types. It has long been the case that more significance is attributed to the shapes of cumulative grain-size curves than to the distribution curves for sediments (e.g., Tricart and Cailleux 1962, Bridge 1981). However, where the details of their form are concerned, grain-size distribution curves are more telling than cumulative ones (Allen and Haslett 2006). The shape of the distribution curve may display various 'features' (F) characteristic of dispersed sediment, and these features are also classified in line with their frequencies of occurrence. The primary (M) and secondary (m) modes have the highest frequencies. Shoulder-like segments (S) are of a lower strength than the primary and secondary modes. Particular features are absent (A) from some samples and unrealized (occluded, O) in others. Augmenting the traditional sand/silt/clay subdivision used in the literature, Manté *et al.* (2007) coined the term colloidal fraction in regard to particle sizes in the range 0.063-1 μm. This fraction is of a geochemical origin.

Grain-size components of eolian deposits in turn depend on the nature of winds blowing (i.e. high- or low-altitude air flows or else near-ground winds), as well as the distances over which transport takes place – long or short (Pye 1987, Tsoar and Pye 1987, Sun *et al.* 2002). On the basis of the feature-related method developed by Allen and Haslett (2006), the descriptive classification from Flemming (2000), and the three reference cumulative curves of eolian types (their transformation toward frequency curves) discussed by Tricart and Cailleux (1962), Essefi (2009) distinguished between three types of eolian sediment. The so-called eolian sand is capable of being transported by strong winds only, its most important features being a mode at 500 μm and shoulders at 250 and 1600 μm. This ensures classification of eolian sediment as sand, in line with the sand/silt/clay diagram of Flemming (2000). Then there is the slightly silty eolian sand (Flemming 2000) which is capable of being transported by even a moderate wind. The most important features in this case are a mode at 315 μm and shoulders at 200 and 800 μm. That leaves silty eolian sand (Flemming 2000) which is even transportable in calm conditions, the most apparent features in this case being a mode at 160 μm and two shoulders at 250 and 1000 μm. To conclude, the fractions centered around 6 and 60 μm (Sun *et al.* 2002), as well as 160, 315 and 500 μm (Essefi 2009) mark the eolian component. The hydraulic component is in turn marked by the 1 and 380 μm fractions (Sun *et al.* 2002). The geochemical fraction is in turn characterized by colloids, with particles of diameters below 1 μm (Manté *et al.* 2007).

Magnetic susceptibility was measured with the aid of a Bartington MS2B probe at the Laboratory of Sedimentary Dynamics and the Environment of the National Engineering School of Sfax, at a frequency of 0.47 kHz. The use of magnetic susceptibility is twofold, it allowing on the one hand for the detection of a high magnetic signature probably related to tephra layers, which may serve in core-dating. The use of magnetic susceptibility in tephrostratigraphy was discussed recently by Essefi *et al.* (2012b). On the other hand, it may also have climatic or sedimentary significance.

RESULTS

RECORD OF THE CLIMATIC VARIABILITY OVER THE LAST TWO MILLENNIA: THE CORRELATION BETWEEN CORES FROM SEBKHAS MHABEUL AND SOUASSI

The response of the Souassi clay pan to climatic variability is manifested either in terms of confinement periods, expressed visually in terms of high major grey scales or else oxygenated periods, expressed through low major grey scales. Major grey-scale variability and three reference sandy bands were thus able to offer a basis upon which to correlate the core of sebkha Mhabeul (SE Tunisia) – as recently published on by Marquer *et al.* (2008), as well as the core from the Souassi clay pan, the aim being to infer climatic variability during the last two millennia.

Chronology and major climatic events seen in the sebkha Mhabeul core

With a view to tephrochronology being supplemented, Marquer *et al.* (2008) used minor grey-scale variability as a proxy in the assessment of climatic variability. Since the purpose is to find this same climatic variability within the Souassi cores, the minor grey scale of the sebkha Mhabeul core, detectable only by image software, is transformed towards the major grey scale (Fig. 2), which may be detected with the naked eye in the sebkha Mhabeul core. The three reference bands are also represented along the core (Fig. 2). The determination of major grey-scale variability thus yields evidence of apparent similarity between the sebkha Souassi core and that from sebkha Mhabeul (Fig. 2). This core, then, is ready to be used as a tool by which to detect climatic stages already recognized in sebkha Mhabeul within the cores from sebkha Souassi. As regards these climatic stages, the tephrochronology has the sebkha Mhabeul core (of 65 cm) covering the last 1700 yr – Figure 2 (Marquer *et al.* 2008). This time interval encompasses six different climatic stages, from top to bottom.

First, in the uppermost 3 cm of the core there is evidence of the Warming Present (WP) stage, extending from (1954–80= 1874) to 1993, i.e. ≈120yr; the establishment of modern conditions is characterised by stability, with a high grey scale. With the addition of a small salt crust, this period is dominated by clayey sedimentation. Second, stage C4 is located between 3 cm and 12.5 cm and is referred to as the **L**ate **L**ittle **I**ce **A**ge (Late LIA) – Wiles *et al.* (2008); it stretches between 80 and 400yrBP, i.e. over 320yr. It is characterized by intermediate GS values; the clayey sedimentation making up twofold and threefold laminates. This period is limited at the bottom by the first reference sandy band extending from 12.5 cm to 15 cm. Third, from ca. 400yrBP to 600yrBP, during the 200 years of cycle C3, which is called the **E**arly **L**ittle **I**ce **A**ge (ELIA), the GS signal attains low values only. As for the grain-size distribution, the sandy sedimentation with a low grey-scale value characterizing depths between 12.5 and 15 cm represents the first reference band to correlate with cores from the Sidi El Hani

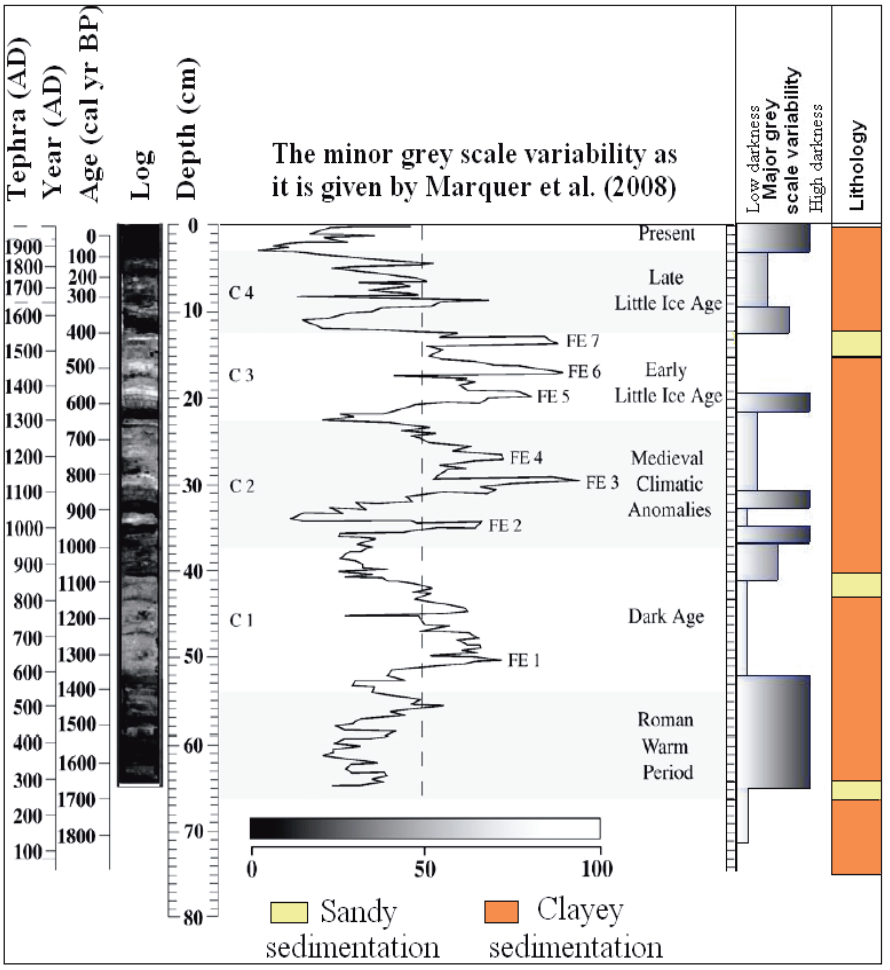

Figure 2. The major gray-scale variability, sandy reference bands, and major climatic events during the last two millennia at sebkha Mhabeul: transformation of minor to major gray-scale variability (Marquer *et al.* 2008: modified)

clay pan; since such sandy bands are rare within such a clay pan. This stage ends at a depth of 23 cm. Fourth, the passage to stage C2, which is called the **M**edieval **C**limatic **A**nomaly (MCA), is marked by a sharp decrease in the GS. The MCA spanned between ca. 600yrBP and 1000yrBP, i.e. ≈400yr. The initiation of this cycle C2 is marked by a sharp decrease in GS values, revealing a return to intense flood activity. The end of this stage (37 cm) is marked by two oscillations of high grey scale. Fifth, during the stage (C1) of the Dark Ages (DA), which stretches from 37 to 54 cm, a shift from light to dark sediments is recorded between ca. 1000yrBP and 1400yrBP, i.e. over 400 years. As for the grain-size distribution, the second reference sandy band is detected at the top of the DA. Sixth, the 300-year **R**oman **W**arm **P**eriod

(RWP) stretches between 1400 and 1750 yrBP. During the RWP, high GS values associated with dark sediments suggest stable climatic conditions with small and/or scarce flood events; this period is recorded in the core from sebkha Mhabeul between 54 and 65 cm. The bottom of this recording is marked by a third sandy reference band between 63 and 65 cm down.

Correlation between the sebkha Mhabeul and Sidi El Hani clay pan cores

The correlation between the core (of 114 cm) from sebkha Souassi and that from sebkha Mhabeul (of length 65 cm) – Figure 3 – shows that the climatic variability recorded during the last two millennia over 65 cm is recorded in the core from sebkha Souassi over 114 cm. The rate of sedimentation is thus higher in this location of sebkha Souassi than at sebkha Mhabeul.

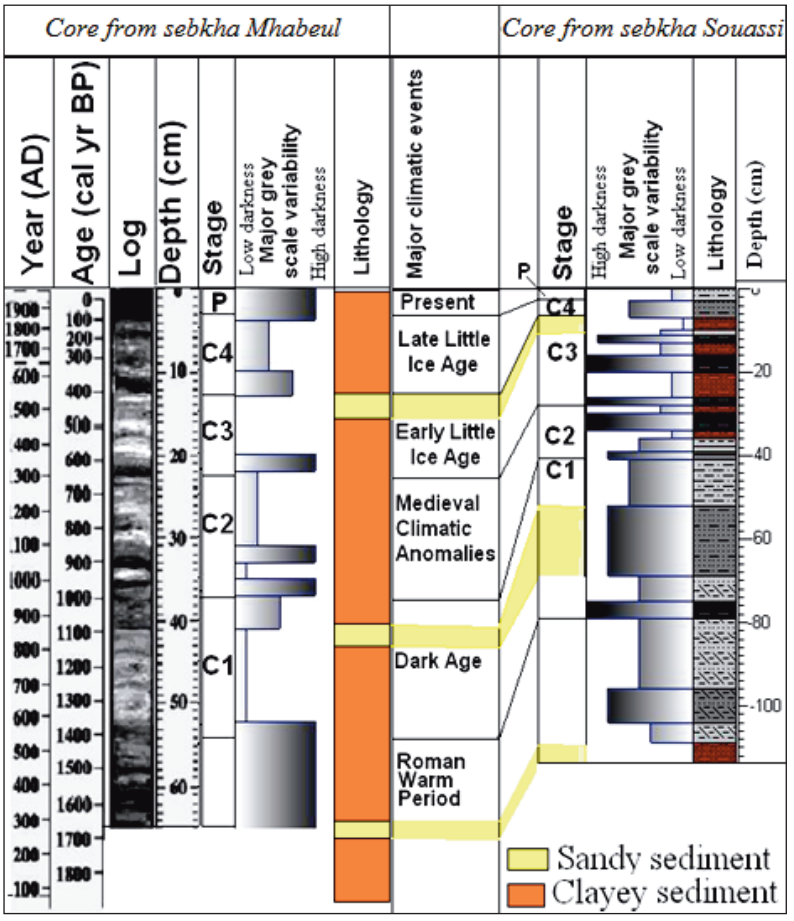

Figure 3. Correlation between sebkhas Mhabeul and Souassi as based on gray-scale variability and the three sandy reference bands

By following the major grey-scale variability and the three reference bands along both cores, the six climatic stages recognized in sebkha Mhabeul were also found along the core from sebkha Souassi. First, the Warming Present (WP) stretches along the uppermost 3 cm with its high grey scale as a sign of a dry climate. Second, the Late Little Ice Age (Late LIA) is located at depths between 3 and 7 cm. As in the case of the sebkha Mhabeul core, this period is delimited from below by the first reference sandy band. Third, the Early Little Ice Age (ELIA) is located between 7 and 28 cm down the core. Climatologically, the intermediate values for the GS indicate that this stage may be classified as moderate. Fourth, the Medieval Climatic Anomaly (MCA) spanning from 28 to 40 cm is marked by a sharp decrease in the GS, revealing a wet period. Fifth, the **D**ark **A**ges (DA) appears along the section from depths between 40 and 79 cm, a shift from light to dark sediments being recorded. As for grain-size distribution, the second reference sandy band is detected at the top of the DA. Sixth, the Roman Warm Period (RWP) appears between 79 and 114 cm down. By reference to the major grey scale, it is possible to divide this period into sub-stages. The first (from 79 down to 109 cm in the sebkha Souassi core) is marked by high GS values associated with the dark sediments suggestive of stable climatic conditions. The second (from 109 down to 114 cm in the sebkha Souassi core) is recorded in the bottom and is marked by a third sandy reference band and low GS values as signs of a wet climate.

THE RECORD OF SEDIMENTARY DYNAMICS AND CLIMATIC VARIABILITY

This work treats magnetic susceptibility as a tool with which to infer the existence of tephra layers. As in the case of previous work (Essefi *et al.* 2013, Essefi 2013), several peaks of magnetic susceptibility values are seen to be located at 4, 75 and 110 cm depths, this probably relating to well-dated volcanic activity (Marquer *et al.* 2008). The presence of these tephras layers is in good concordance with the tephras located at sabkha Boujmal, eastern Tunisia (Essefi and Yaich 2013).

Mean grain-size distribution values and magnetic susceptibility may be used as a basis for sub-dividing the core from sebkha Souassi into different progradational and retrogradational cycles. This cyclicity is governed by the interplay of local tectonic activity and water-table fluctuations (Essefi 2013, Essefi *et al.* 2013) on the one hand, and by global change in climatic conditions on the other.

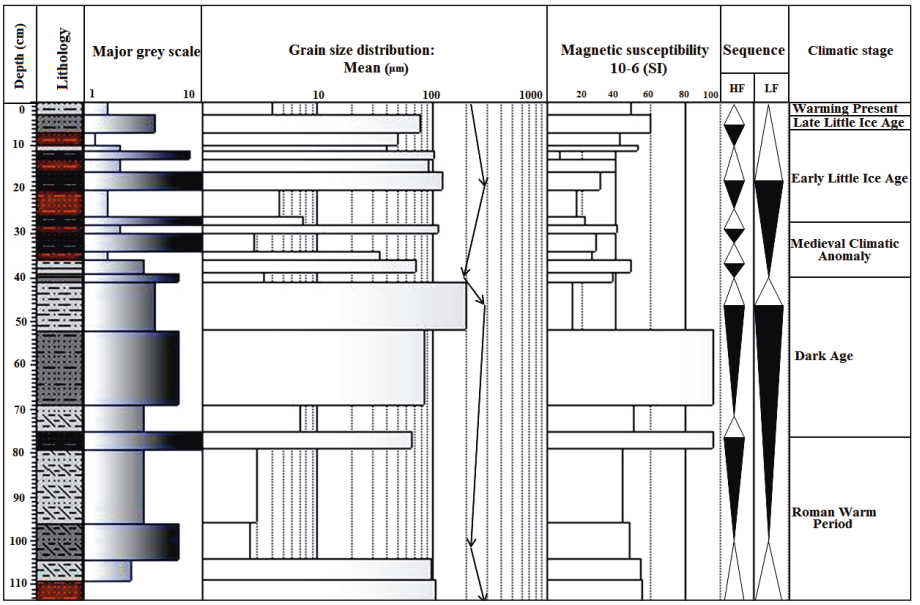

Figure 4. Mean grain-size distribution, magnetic susceptibility and cyclostratigraphy down the core from sebkha Souassi

The Warming Present (WP) and Late Little Ice Age (Late LIA)

The WP period is dominated by a clayey sedimentation. The top of the cycle (Fig. 5a) displays obvious fining; it is characterized by a primary mode (M: ca 7 µm) as an indication of fine eolian sedimentation. The secondary mode (M: less than 0.1 µm) is in turn indicative of geochemical sedimentation. The geochemical and eolian fractions prevail over hydraulic sedimentation. Second, there is stage C4 located between 3 and 12.5 cm and relating to the Late Little Ice Age (Late LIA) – Wiles *et al.* (2008). This stretched between 80 and 400yrBP, i.e. over a period of 320yr. It is characterized by intermediate GS values; the clayey sedimentation making up double or triple laminates. This period is limited at the bottom by the first reference sandy band at depths between 12.5 and 15 cm. The Late Little Ice Age (Late LIA) is manifested in an increase in the fine eolian fraction and a decrease of the geochemical and hydraulic fractions (Fig. 5b). It is characterized by a primary mode (M: ca 160 µm) indicative of coarse hydraulic sedimentation, as well as by a translated secondary mode (M: ca 10 µm) as an indication of fine eolian sedimentation, and an absent (A: ca 20–80 µm).

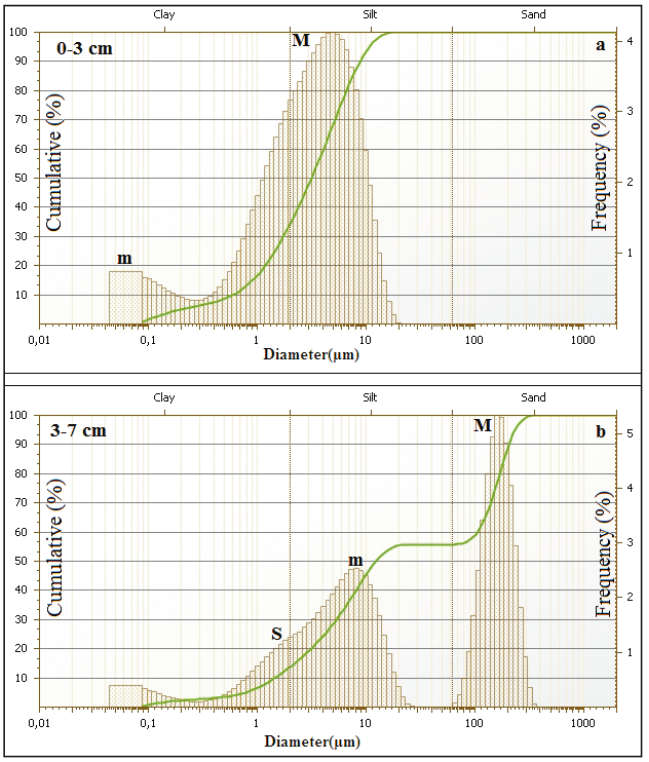

Figure 5. Grain-size distribution for the WP and Late LIA along the core from sebkha Souassi

Early Little Ice Age

The bottom of this period (Fig. 6e,f) is expressed by a very fine sedimentation, which coincides with the minimum of accommodation. The decrease in accommodation reflects stable climatic conditions and/or a water table rise. The middle of the period represents the maximum level of accommodation. In a process reflecting stable climatic conditions and/or a water-table fall. The low-frequency progradational cycle at the top of the core is expressed by an upward trend for the fine eolian fraction, and by a decrease in the role played by the geochemical and hydraulic fractions (Fig. 6c,d,e,f). It is between 12.5 and 15 cm below the surface that the first reference band manifests itself (Fig. 6c). It is characterized by a primary mode (M: ca 160 µm) indicative of coarse eolian sedimentation, a translated secondary mode (m: ca 10 µm) indicating the fine eolian sedimentation, and an absent (A: ca 30–60 µm). The second sample of the maximum accommodation (Fig. 6d) is characterized by the same features. Nevertheless, it typically has the more obvious shoulder (S: ca 2 µm) indicating fine hydraulic sedimentation.

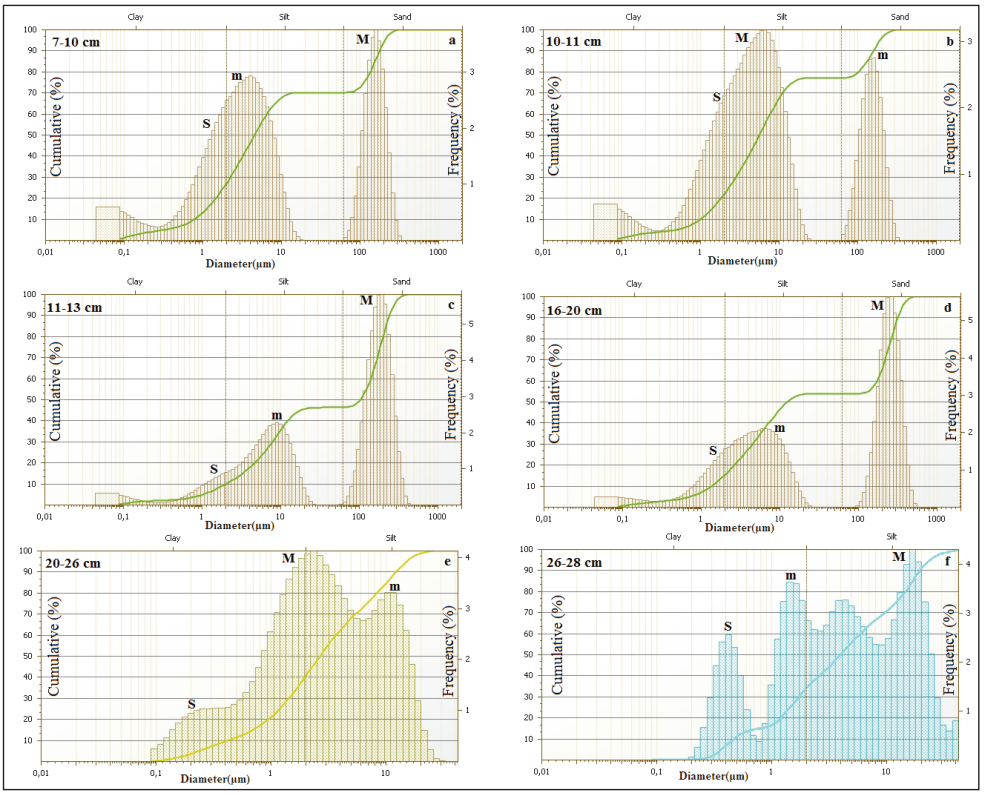

Figure 6. Grain-size distribution for the Early Little Ice Age along the core from sebkha Souassi

Medieval Climatic Anomaly (MCA)

The MCA is marked by a downward trend for size in the grain-size distribution (Fig.7 a,b,c,d,e), followed by a sharp increase in GS. The top of the cycle (Fig. 7a) shows an obvious coarsening with a primary mode (M: ca 160 µm) indicatinh coarse eolian sedimentation, as well as a translated secondary mode (M: ca 10 µm) indicative of fine eolian sedimentation, and an absent (A: ca 30–70 µm). Downward (Fig. 7b), the sedimentation becomes finer. Geochemical and hydraulic fractions come to prevail, at the expense of fine eolian sedimentation. These two samples form a progradational cycle of high order (Fig. 4), which is preceded by a retrogradational cycle of high order encompassing the two coarse samples (Fig. 7c,d). The bottom of the low-frequency progradational cycle (Fig. 7e) is characterized by a primary mode (M: ca 7 µm).

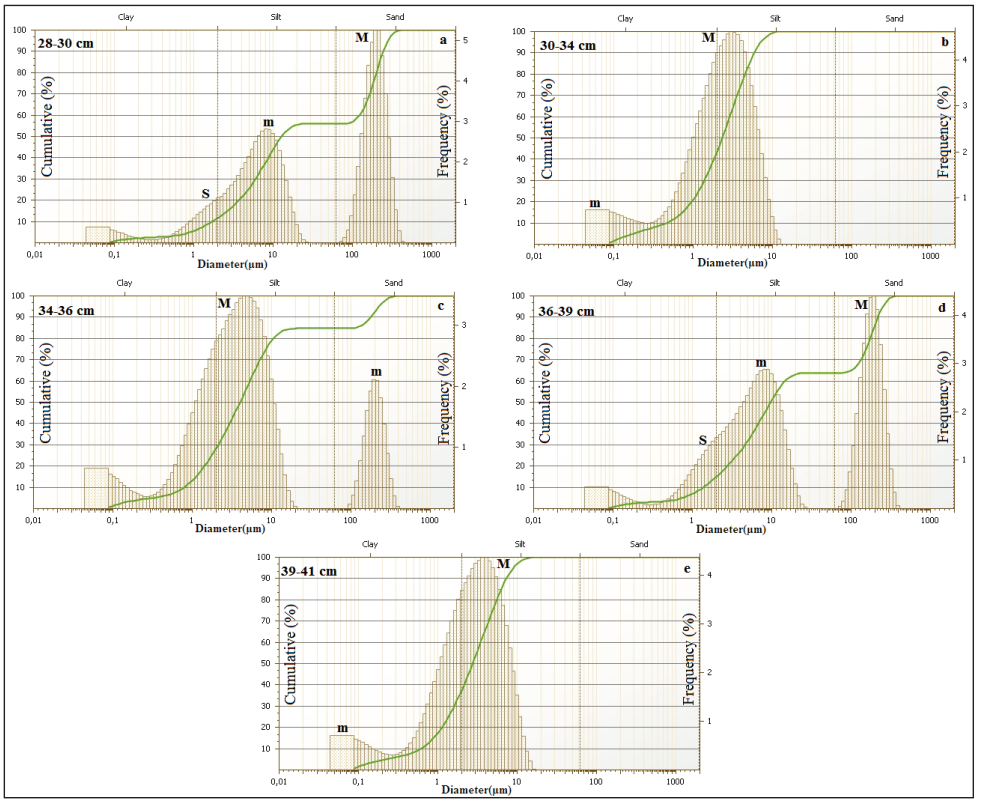

Figure 7. Grain-size distribution of the Medieval Climatic Anomaly along the core from sebkha Souassi

Dark Ages (DA)

This period shows a downward trend for size where grain-size distribution is concerned. The low-frequency progradational cycle at the top of the core is expressed through increased importance of the fine eolian fraction and decrease reduced role for the geochemical and hydraulic fractions (Fig. 8b,c). The top of the cycle (Fig. 8a) shows an obvious coarsening (Mean: 3.35 µm); it is characterized by a primary mode (M: ca 2 µm) indicating the fine hydraulic sedimentation, a translated secondary mode (M: ca 40 µm) indicating the fine eolian sedimentation, and an absent (A: ca 100–2000 µm). The second sample (Fig. 8b) is characterized by the same features and similar sizes (Mean: ca 3.2 µm). Nevertheless, sizes are less dispersed around the mode than was the case for the previous sample. Downwards (Fig. 8c,d), the sedimentation becomes finer (Means: ca 2.66 and 2.1 µm) and more centered around the modes. The geochemical and hydraulic fractions come to prevail, at the expense of the fine eolian sedimentation.

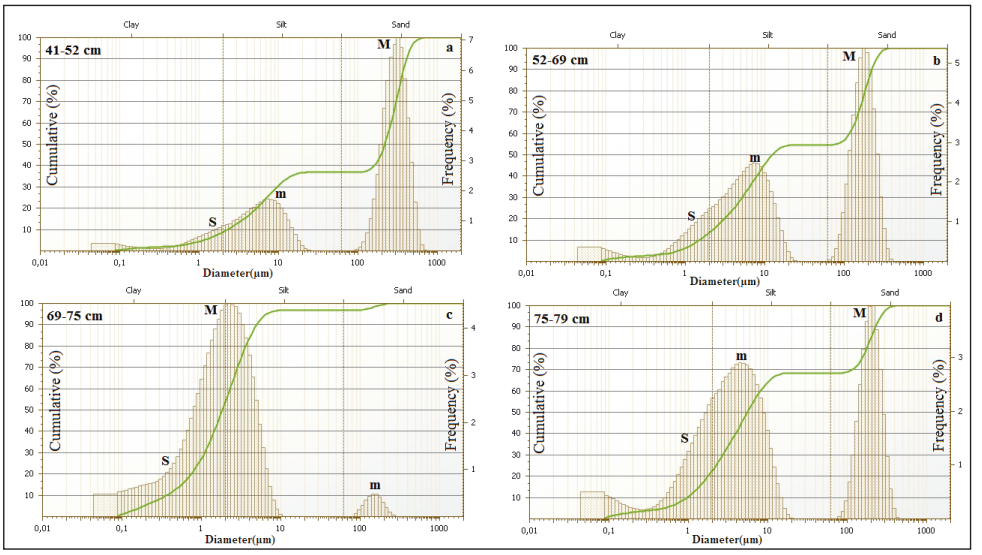

Figure 8. Grain-size distribution for the Dark Ages along the core from sebkha Souassi

Roman Warm Period

This period shows a downward trend for size where grain-size distribution is concerned. The low-frequency progradational cycle at the top of the core is manifested in increased importance of the fine eolian fraction, as well as a reduction in the geochemical and hydraulic fractions (Fig. 9b,c). The top of the cycle (Fig. 9a) shows an obvious coarsening (Mean: 3.35 µm); it is characterized by a primary mode (M: ca 2 µm) as an indication of fine hydraulic sedimentation, a translated secondary mode (M: ca 40 µm) indicating fine eolian sedimentation, and an absent (A: ca 100–2000 µm). The second sample (Fig. 9b) is characterized by the same features and a similar size (Mean: ca 3.2 µm). Nevertheless, it is less dispersed around the mode than the previous sample. Downward (Fig. 9c,d), the sedimentation becomes finer (Means: ca 2.66 and 2.1 µm) and more centered around the modes. The geochemical and hydraulic fractions prevail there at the expense of fine eolian sedimentation.

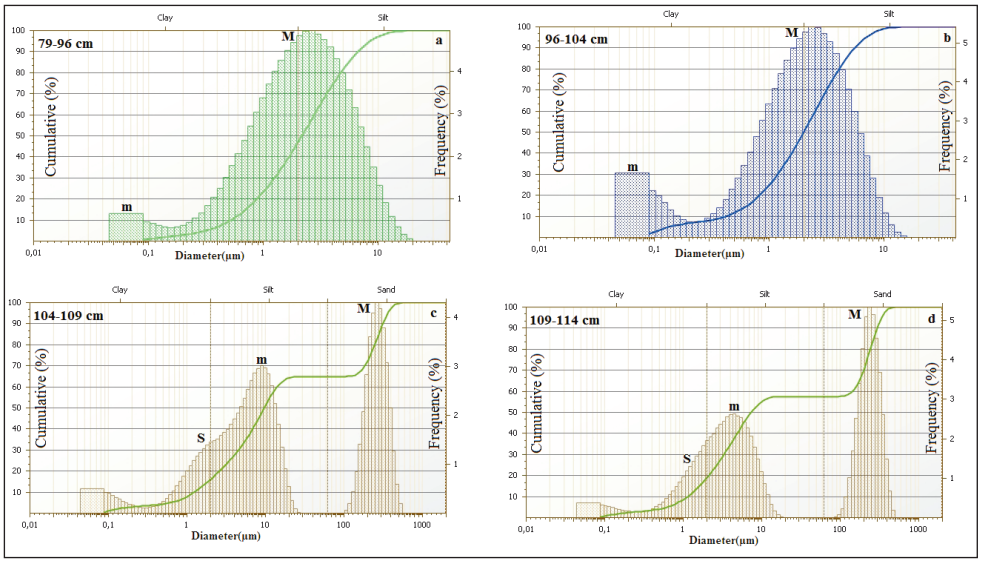

Figure 9. Grain-size distribution of the Roman Warm Period along the core from sebkha Souassi

CONCLUSIONS

The Tunisian geomorphological feature known as sebkha Souassi can offer a record as regards the variability of both sedimentary dynamics and climate. VCD proved to be a useful tool by which to analyse correlations between cores from sebkhas Souassi and Mhabeul, with a view to climatic variability over the last two millennia being inferred from the geology of this clay pan. High values for magnetic susceptibility in turn allow for the detection of probable levels of tephras. The method permits the inferring of climatic variability affecting the Souassi saline environment over the last two millennia. The six climatic stages recognized from the sebkha Mhabeul core were also identifiable in the core from the Souassi clay pan. As for the three sandy reference bands, each belongs to a different climatic stage. In all the cores, the first sandy reference band is detected in the Early Little Ice Age (ELIA), while the second is in the Roman Warm Period (RWP) and the third in the Dark Ages (DA). Furthermore, the Souassi core attests to sebkha Souassi subsiding more than sebkha Mhabeul. The aforesaid climatic stages are combined with radical change in sedimentary dynamics detected by way of the genetic study of grain-size distribution.

REFERENCES

Allen J.R.L., Haslett S.K., 2006, *Granulometric characterization and evaluation of annually banded mid-Holocene estuarine silts, Welsh Severn Estuary (UK): coastal change, sea level, and climate*, Quaternary Science Reviews, 25, 1418–1446.

Ben Jmaa H., 2008, *The endorheic system of Sidi El Hani, Chrita and Mechertate: Paleoenvironment and recent dynamics*, PhD Thesis, University of Tunis.

Bridge J.S., 1981, *Hydraulic interpretation of grain-size distributions using a physical model for bedload transport*, Journal of Sedimentary Petrology, 51, 1109–1124.

Essefi E., 2009, *Multidisciplinary study of Sidi El Hani Saline Environment: the History and the Climatic Variability*, Master thesis, Faculty of sciences of Sfax, University of Sfax.

Essefi E., 2013, *Wet Aeolian Sedimentology and Sequence Stratigraphy in Eastern Tunisia: Implications for Wet Aeolian Sedimentology and Sequence Stratigraphy on Mars*, Ph.D, thesis, National Engineering School of Sfax.

Essefi E., Fairén A. G., Komatsu G., Rekhiss F., Yaich C., 2012a, *Study of cores from a spring mound at the mars analog of Boujmal, eastern Tunisia: coring martian spring mounds as potential efficient tool for a geologic exploration of early Mars*, Third Conference on Early Mars, 7029 (abstracts).

Essefi E., Komatsu G., Fairén A.G., Rekhiss F., Yaich C., 2012b, *Identification of tephra layers in spring mounds at the terrestrial analog of Boujmal, eastern Tunisia: repercussions and limits of tephrostratigraphy application on martian stratigraphy and paleoclimatology*, Third Conference on Early Mars, 7034 (abstracts).

Essefi E., Komatsu G., Fairén A.G., Chan M. A., Yaich, C., 2013, *Groundwater influence on the aeolian sequence stratigraphy of the Mechertate-Chrita-Sidi El Hani system, Tunisian Sahel: Analogies to the wet-dry aeolian sequence stratigraphy at Meridiani Planum, Terby crater, and Gale crater, Mars*, Accepted manuscript, Planetary and Space Science, DOI: 10.1016/j.pss.2013.05.010.

Essefi E., Touir J., Tagorti M.A., Bouri S., Essefi H., Ouali J., Ben Jmaa H., 2009, *Modeling of the chaotic behavior of Sidi El Hani discharge playa, Tunisian Sahel: which exogenous factor commands this saline environment? The subsurface flow or the climatic variability?* International Congress Geotunis, 4th edition.

Essefi E., Touir J., Tagorti M.A., Yaich C., 2012c, *Effect of the groundwater contribution, the climatic change, and the human induced activities on the hydrological behavior of discharge playas: a case study Sidi El Hani discharge playa, Tunisian Sahel*, Arabian Journal of Geoscience, DOI: 10.1007/s12517-012-0659-6.

Essefi E., Touir J., Tagorti M.A., Yaich C., 2013, *Magnetic Study of the Sedimentary Filling of Sebkha Boujmal, (eastern Tunisia): the Sedimentary Dynamics and the Climatic Variability,* International Conference on Natural Hazard and Geomatics (ICNHC), 17–20 May, Hammamet, Tunisia.

Flemming B.W., 2000, *A revised textural classification of gravel-free muddy sediments on the basis of ternary diagrams*, Continental Shelf Research, 20, 1125–1137.

Manté C., Yao A.F., Degiovanni C., 2007, *Principal component analysis of measures, with special emphasis on grain-size curves*, Computational Statistics & Data Analysis, 51, 4969–4983.

Marquer L., Pomel S., Abichou A., Schulz E., Kaniewski D., Van Campo E., 2008, *Late Holocene high resolution palaeoclimatic reconstruction inferred from Sebkha Mhabeul, southeast Tunisia*, Quaternary Research, 70, 240–250.

Mefteh S., Essefi E., Medhioub M., Yaich C., Jamoussi F., 2012, *Correlation between clay minerals, organic matter, and magnetic susceptibility along NWA-1 well (southern Tunisia): paleo-environmental indications*, 4th Magrebian Symposium on Clays, 21–23 March, Hammamet, Tunisia, Abstract book, pp. 78.

Pye K., 1987, *Aeolian dust and dust deposits*, Academic Press, London, 29–62.

Rodbell D.T., Seltzer G.O., Anderson D.M., Abbott M.B., Enfield D.B., Newman J.H., 1999, *An 15,000-year record of El Niño-driven alluviation in southwestern Ecuador*, Science 283, 516–520.

Sun D., Bloemendal J., Rea D.K., Vandenberghe J., Jiang F., An Z., Su R., 2002, *Grain-size distribution function of polymodal sediments in hydraulic and aeolian environments, and numerical partitioning of the sedimentary components,* Sedimentary Geology, 152, 263–277.

Tagorti M. A., Essefi E., Touir J., Guellala R., Yaich C., 2013, *Geochemical controls of groundwaters upwelling in saline environments: Case study the discharge playa of Sidi El Hani (Sahel, Tunisia)*, Accepted manuscript, African Earth Science Journal.

Tricart J., Cailleux A., 1962, *Le modèle glaciaire et nival, SEDES*, Paris.

Tricart J., Cailleux A., 1967, *Le modelé des régions périglaciaires, SEDES*, Paris.

Tsoar H., Pye K., 1987, *Dust transport and the question of desert loess formation*, Sedimentology, 34, 139–153, doi:10.1111/j.1365-3091.1987.tb00566.x.

Wiles, G.C., Barclay, D.J., Calkin, P.E., Lowell, T.V., 2008, *Century to millennial-scale temperature variations for the last two thousand years indicated from glacial geologic records of Southern Alaska*, Global and Planetary Change, 60, 115–125.